NASA
Technical Memorandum 82623

AVRADCOM
Technical Report 81-C-14

A Method of Selecting Grid Size to Account for Hertz Deformation in Finite Element Analysis of Spur Gears

John J. Coy
Propulsion Laboratory
AVRADCOM Research and Technology Laboratories
Lewis Research Center
Cleveland, Ohio

and

Charles Hu-Chih Chao
Northwestern University
Evanston, Illinois

Prepared for the
Design Engineering Technical Conference
sponsored by the American Society of Mechanical Engineers
Hartford, Connecticut, September 20-23, 1981

NASA

A METHOD OF SELECTING GRID SIZE TO ACCOUNT FOR HERTZ DEFORMATION IN FINITE ELEMENT ANALYSIS OF SPUR GEARS

by John J. Coy*

Propulsion Laboratory
AVRADCOM Research and Technology Laboratories
NASA Lewis Research Center
Cleveland, Ohio 44135

and

Charles Hu-Chih Chao**

Northwestern University
Evanston, Illinois 60201

E-728

ABSTRACT

A method of selecting grid size for the finite element analysis of gear tooth deflection is presented. The method is based on a finite element study of two cylinders in line contact, where the criterion for establishing element size was that there be agreement with the classical Hertzian solution for deflection. Many previous finite element studies of gear tooth deflection have not included the full effect of the Hertzian deflection. The present results are applied to calculate deflection for the gear specimen used in the NASA spur gear test rig. Comparisons are made between the present results and the results of two other methods of calculation. The results have application in design of gear tooth profile modifications to reduce noise and dynamic loads.

SYMBOLS

b width of Hertzian flat, m (in.)

c,e dimensions of finite elements

d diameter

---

*Member ASME.

**Presently with Garrett Turbine Engine Co., Phoenix, Arizona 85010.

E Young's modulus, N/m^2 (psi)

p load per unit length, N/m (lb/in.)

r_b base circle radius, m (in.)

s distance measured along involute from pitch point, m (in.)

x,y Cartesian coordinates

δ deflection, m (in.)

θ roll angle, deg

ν Poisson's ratio

ρ radius of curvature, m (in.)

ϕ pressure angle, deg

INTRODUCTION

Gear tooth deflections in heavily-loaded, high-speed power transmissions cause noise. When a loaded tooth deflects in the direction of the load, this displaces the tooth from a proper geometrical position for smooth gear action. When the next tooth comes into mesh it is effectively ahead of where it should be. The premature contact of the tooth coming into mesh causes an impact or dynamic load, which in turn produces noise in the gear transmission.

If the deflection of the tooth under load can be predicted with good accuracy, then appropriate geometrical compensations may be designed into the gear to eliminate noise. Since deflection is a function of load, any remedy such as a geometrical correction to the tooth would be effective at a given condition of design load. The traditional design practice has been to specify a straight line involute correction from the tip of the tooth to the highest point of single tooth pair contact. The amount of correction is made equal to the calculated deflection. In 1929 Baud and Peterson [1][1]

---

[1]Numbers in square brackets denote references at end of paper.

approached the gear tooth deformation problem by modeling the gear tooth as a cantilever beam with variable cross-section. In 1938 Walker [2] related gear tooth deflections to tooth profile modification to achieve smooth running gear meshes. His very useful results are still being followed by some gear designers today.

In more recent times there have been efforts to improve the accuracy of calculating the deflection of gear teeth by considering all contributing sources such as bending, shear, and compressional deflections of the gear teeth as well as deformations due to flexibility of the gear blank and mounting. These efforts make use of the early work of Weber [3], adding various improvements. In 1964 Attia [4] contributed the effect of rim stiffness. In 1980 Cornell [5] presented the accumulation of his research on the subject. His work is based on classical treatments of tooth deformation due to the effects of bending, shear, Hertzian deformation, fillet geometry, and foundation flexibility.

There have been recent studies of gear system dynamics and gear tooth deformation based on finite element analysis of gear teeth [6 to 8], but the complete effect of Hertzian deformation does not seem to be included. It will be shown in a later section that the Hertzian deformation component of total gear tooth deformation can be as much as 25 percent of the total deformation. This means that in any finite element calculation of gear tooth deformation, the grid spacing in the zone of the tooth to tooth contact must be chosen carefully. In many finite element studies in the literature cited this point has been overlooked.

The most recent studies of gear dynamic load prediction have been by Cornell and Westervelt [9], Wallace and Seireg [6], and Kasuba and Evans [10]. Wang and Cheng [11] have presented a research study on combined dy-

namic load, lubrication film thickness, and temperature analysis of spur gear sets. Mark [12 to 14] has studied gear noise using Fourier analysis of the steady and random components of the static transmission error. Remmers [15] has also presented a frequency domain approach to the problem of gear mesh dynamics and noise.

The objectives of the work presented herein were to (a) derive a method of selecting finite element grid size so that the full effect of Hertzian deformations would be included, (b) apply the method to calculate tooth deflections for the spur gear specimens in the NASA spur gear test rig, and (c) compare the results with those of Wang and Cheng [11] and Cornell [15]. The method of [13] was used to select the design load.

ANALYSIS

A finite element study of a cylinder was conducted in order to determine what grid spacing was necessary to get correct answers for the Hertzian component. The cylinder problem was chosen because the geometry of line contact is similar to the line contact between two gear teeth. In addition, the equations for Hertzian deformation of cylinders are well known. These are summarized in the appendix. The essentials of the finite element method are presented in [6].

The finite element work was done using the MARC program [17] at the NASA Lewis Research Center. A plane strain 8-node distorted quadrilateral element was selected. Due to symmetry, only one half of the cylinder was modeled as shown in Fig. 1. A fine grid was used in the Hertzian contact zone. This was to allow the stress field to dampen down according to the St. Venant principle [18]. The boundary conditions on the half cylinder is no y-displacement along $y = 0$ line and at the point (0,0) there must be no deflection.

The question to be answered was, is the fine mesh region large enough to allow the strain field to dampen out according to the St. Venant principal? Or in other words, for the range of mesh size to be used, how far away from the point load should the fine mesh zone be extended? In order to answer the question, the fine mesh zone was modeled with three different mesh arrangements. These are shown in Fig. 2. The edge of the zone along the circumference was consistently divided into 9 divisions, while the radial direction was divided into 3, 5, and 10 divisions for each case. Table I gives the displacements at the four nodes A, B, C, and D shown in Fig. 1. Because there is symmetry about the y-axis, the displacements at G, F, and E are the same as A, B, and C. Because the displacements at A, B, C, and D are not significantly infuenced by the mesh arrangement within the small mesh zone it is safe to conclude that the small mesh zone is large enough.

The load distribution on a Hertzian contact is parabolic. In the finite element model, the load must be applied at discrete points. Two methods of approximating the parabolic load distribution were used. One method was to apply the load at several closely spaced points in the contact zone. A second method was to apply the load at one node only. The latter method called the concentrated load method is discussed next.

Concentrated Load Approach

The result of the finite element calculations using concentrated loads are compared with results from the Hertzian deflection formula, Eq. (A1). The comparison is summarized in Fig. 3. The results show that as the grid size in comparison to the Hertzian contact width is increased, the percent error monotonically decreases, passing through zero. The percent error is taken as

$$\text{Percent error} = \frac{\delta_f - \delta_h}{\delta_h} \times 100 \tag{1}$$

where δ_f is the deformation calculated by the finite element method, and δ_h is the deformatioan calculated from the Hertzian formula given in the appendix. The grid spacing that gives zero percent error depends on the grid aspect ratio. The aspect ratio (c/e) is defined as the ratio of the element dimension (in the direction normal to the loaded edge) to the element size (which is measured along the loaded edge). As the aspect ratio decreases, the ratio of element size to contact width must increase to maintain a zero percent error. The following equation derived from Fig. 3 relates element size and aspect ratio, giving less than 1 percent error in calculated deflection within the interval of definition

$$\left(\frac{e}{b}\right) = -0.2\left(\frac{c}{e}\right) + 1.2, \quad 0.9 < \frac{c}{e} < 3 \tag{2}$$

The results of this preliminary study enables the selection of grid spacing for the gear tooth finite element model, when a concentrated load is used to represent the gear tooth contact. By selecting the proper grid size and aspect ratio the Hertzian contact deformation will be accurately calculated.

The procedure for selecting a mesh spacing along the loaded edge of a gear tooth would then be as follows. From Eq. (A5) determine the point of the involute at which the load acts. From Eqs. (A6) and (A3) determine the Hertzian contact width b. Then from Eq. (2) select the element size, e, given that the aspect ratio, c/e, has been selected beforehand.

Distributed Load Approach

A distributed load approach was also investigated for calculation of the Hertzian deformation of cylinders in contact.

In the finite element approach the distributed load on a surface leads to the numerical evaluation of a surface integral. By performing the numerical integration, the appropriate concentrated loads to be assigned to the nodes of the element are determined. This numerical integration is handled automatically by most computer codes and in particular by the MARC Code used in this investigation.

The grid spacing was varied and computed finite element deflections were compared to calculated Hertzian deflections in a way similar to that shown in Fig. 3. The variation in percent error with ratio of element size to contact width did not vary monotonically. Also the percent error variations were beyond an acceptable limit of 10 percent. The results obtained from the distributed load method did not provide a satisfactory way to select element size to minimize the error.

RESULTS AND DISCUSSION

Using the analysis of the previous section the finite element method was used to calculate deflections of the spur gear which is used in the NASA spur gear test rig. The test rig is described in [19]. Table II gives the dimensions of the test gears. For the calculations the fillet radius was taken as 0.102 cm (0.04 in.).

The load pattern used in the finite element calculations was selected on the basis of the method of Mark [13]. The maximum load along the line of action is the test load of 1615 N (363 lb). The complete load pattern is shown in Fig. 4. The abscissa is the roll angle as defined by Baxter in [20]. For the true involute profile gear running against an identical gear

the active zone is 21.0601 degrees, beginning at 10.3239 degrees of roll angle. The zone of no load at the addendendum and dedendenum of 2.0959 degrees according to Mark[2] is to allow for tooth tip relief, 20 percent overloading, and possible tooth spacing errors. The object of using this load pattern was to obtain the tooth deflections under the loading which according to [13] leads to optimum reduction of tooth mesh generated noise.

The mesh for the finite element analysis is shown in Fig. 5. The mesh size was determined using the analysis presented earlier.

Table III and Fig. 6 give the deflections which were calculated for 30 different points along the tooth profile. The trapezoidal shape of the deflections plotted in Fig. 6 is reflective of the trapezoidal shape of the applied loads as shown in Fig. 4. The deflections are larger for loading in the addendum region due to greater bending of the tooth.

There are other analyses of gear tooth deflection which may be compared to the results presented in Table III. In [11], Wang and Cheng calculated deflection for a spur gear with a normal load applied at various points along the tooth profile. The mesh used by Wang and Cheng for the gear tooth was more coarse than that used in the present study; the boundary constraints and hub size were similar. In [5], Cornell presented a general analysis of tooth deflection. The result of Wang and Cheng and Cornell are compared in the present results in Fig. 7. The present work gives larger deflections than the other two. A possible explanation of why the result of Wang and Cheng gives smaller deflections than the present result can be reasoned from Fig. 3.

Wang and Cheng used an e/b larger than one. Figure 3 shows that this would result in a deformation less than that predicted by Eq. (A1). The

---

[2]Private communication.

authors can not offer any explanation of the difference between Cornell's result and the present result, since the two methods are quite different.

An advantage of the Cornell method over the finite element method is that Cornell's method gives the deflection components, which are the deflection componet due to Hertzian deformation, beam (shear and bending) effects for the involute portion of the tooth, beam effects for the undercut length and for the fillet zone, as well as foundation flexibility. The foundation flexibility represents the effect of the gear blank in supporting the tooth. Figure 8 gives the tooth deflection components that were calculated using Cornell's method. This figure shows that Hertzian deflection is approximately 25 percent of the total tooth deflection. This emphasizes the importance of the effect of mesh size in a finite element study of gear tooth deflections.

SUMMARY OF RESULTS

A method of selecting grid size near the point of load application for a finite element study of gear tooth deflection was presented. The method was based on a finite element study of two cylinders in contact wherein the grid size was varied. The finite element results of the cylinder contact problem were compared to results from the classical Hertzian formula. From this a method was established for determining the grid size in a gear contact problem. The method was applied to calculated deflections in the NASA test gear. The calculated deflections were compared to calculated deflections by the method of Wang and Cheng who used the finite element method. A comparison was made using Cornell's method which is not based on the finite element method. The following results were obtained.

1. Accurate finite element method calculation of Hertzian deflection between two cylinders is dependent on (a) the element size in relation to the Hertzian contact width and (b) the element aspect ratio.

2. For agreement between deflection calculated using the finite element method and deflection calculated using the Hertzian formula the ratio of element size to contact width, e/b should be related to grid aspect ratio c/e by the following equation

$$\frac{e}{b} = -0.2\left(\frac{c}{e}\right) + 1.2,\ 0.9 < \frac{c}{e} < 3$$

3. Calculated gear tooth deflections using the grid selection method compared favorably with results of other researchers. The present method gave deflections from 10 to 20 percent greater than the two methods with which it was compared.

APPENDIX - SUMMARY OF CONTACT STRESS AND DEFORMATION FORMULAE FOR GEARS AND CYLINDERS

Hertz [2] has derived formulae for stress and deflections of solid elastic bodies in contact. Roark's handbook [22] gives a summary of deflection formulae that are basd on a Hertz pressure distribution.

For the case of two identical cylinders pressed into contact, the distance between the cylinders is reduced by

$$\frac{2p(1-\nu^2)}{\pi E}\left[\frac{2}{3}+2\ln\left(\frac{2d}{b}\right)\right] \tag{A1}$$

where

p Load per unit length

ν Poisson's ratio

E Young's modulus

d diameter

b total contact width

The total contact width b is given by

$$b = 2.15\sqrt{\frac{pd}{2E}} \tag{A2}$$

where $\nu = 0.3$.

For the case of two gear teeth in contact the width of contact b is given by

$$b = 2.15\sqrt{\frac{pK_D}{E}}$$

where

$$K_D = \frac{2\rho_1\rho_2}{\rho_1 + \rho_2} \tag{A4}$$

and ρ_1, ρ_2 are the radii of curvature of gear tooth 2 and gear tooth 2 at the point of contact.

For two identical gears in mesh the distance along the contact path from the pitch point is given by

$$s = r_b\theta \tag{A5}$$

where r_b is the base circle radius and θ is the angle of gear rotation at the pitch point $\theta = 0$. The expression for K_D in this case is given by

$$K_D = r_b \tan\phi\left[1 - \left(\frac{s}{r_b \tan\phi}\right)^2\right] \tag{A6}$$

where ϕ is the pressure angle.

REFERENCES

1. Baud, R. V. and Peterson, R. E., "Load and Stress Cycle in Gear Teeth," Mechanical Engineering, Vol. 51, No. 9, Sep. 1929, pp. 653-662.

2. Walker, H., "Gear Tooth Deflection and Profile Modification. - Part 1," The Engineer, Vol. 166, No. 4318, Oct. 14, 1938, pp. 409-412; Part 2, Vol. 166, No. 4319, Oct. 21, 1938, pp. 434-436; Part 3, Vol. 170, No. 4414, Aug. 16, 1940, pp. 102-104.

3. Weber, C., "The Deformation of Loaded Gears and the Effect on Their Load-Carrying Capacity," Sponsored Research (Germany), British Scientific and Industrial Research, London, Report No. 3, 1949.

4. Attia, A. Y., "Deflection of Spur Gear Teeth Cut in Thin Rims," Journal of Engineering for Industry, Vol. 86, No. 4, Nov. 1964, pp. 333-342.

5. Cornell, R. W., "Compliance and Stress Sensitivity of Spur Gear Teeth," Journal of Mechanical Design, Vol. 103, No. 2, April 1981, pp. 447-459.

6. Wallace, D. B. and Siereg, A., "Computer Simulation of Dynamic Stress, Deformation, and Fracture of Gear Teeth" Journal of Engineering for Industry, Vol. 95, No. 4, Nov. 1973, pp. 1108-1114.

7. Wilcox, L. and Coleman, W., "Application of Finite Elements to the Analysis of Gear Tooth Stresses," ASME Paper 72-PTG-30, Oct. 1972.

8. Chabert, G., Dang Tran, T., and Mathis, R., "An Evaluation of Stresses and Deflection of Spur Gear Teeth Under Strain," Journal of Engineering for Industry, Vol. 96, No. 1, Feb. 1974, pp. 85-93.

9. Cornell, R. W. and Westervelt, W. W., "Dynamic Tooth Loads and Stressing for High Contact Ratio Spur Gears," Journal of Mechanical Design, Vol. 100, No. 1, Jan. 1978, pp. 69-76.

10. Kasuba, R. and Evans, J. W., "An Extended Model for Determining Dynamic Loads in Spur Gearing," Journal of Mechanical Design, Vol. 103, No. 2, April 1981, pp. 398-409.

11. Wang, K. L. and Cheng, H. S., "Thermal Elastohydrodynamic Lubrication of Spur Gears," NASA CR 3241, Feb. 1980.*

12. Mark, W. D., "Analysis of the Vibratory Excitation of Gear Systems: Basic Theory," Journal of the Acoustical Society of America, Vol. 63, No. 5, May 1978, pp. 1409-1430.

13. Mark, W. D., "Analysis of the Vibratory Excitation of Gear Systems. II: Tooth Error Representations, Approximations, and Application," Journal of the Acoustical Society of America, Vol. 66, No. 6, Dec. 1979, pp. 1758-1787.

14. Mark, W. D. and Fischer, R. W., "Gear Meshing Action as a Source of Vibratory Excitation," Symposium, on Internal Noise in Helicopters, University of Southampton, England, 1980, pp. C2.1-C2.13.

15. Remmers, E. P., "Gear Mesh Excitation Spectra for Arbitrary Tooth Spacing Errors, Load and Design Contact Ratio," Journal of Mechanical Design, Vol. 100, No. 4, Oct. 1978, pp. 715-722.

16. Bathe, K. J. and Wilson, E. L., "Numerical Methods in Finite Element Analysis," Printice-Hall, Englewood Cliffs, N. J., 1976.

17. "MARK General Purpose Finite Element Analysis Program, User Manual, Vols. A and B," MARC Analysis Research Corp., 1979.

---

*Also published as "A Numerical Solution to the Dynamic Load, Film Thickness and Surface Temperatures in Spur Gears, Part I - Analysis, and Part II - Results," Journal of Mechanical Design, Vol. 103, No. 1, Jan. 1981, pp. 177-194.

18. Timoshenko, S. and Goodier, J. N., Theory of Elasticity, 2nd ed., McGraw-Hill, New York, 1951.

19. Townsend, D. P., Coy, J. J., and Zaretsky, E. V., "Experimental and Analytical Load-Life Relation for AISI 9310 Steel Spur Gears," Journal of Mechanical Design, Vol. 100, No. 1, Jan. 1978, pp. 54-60.

20. Dudley, D. W., ed., Gear Handbook, 1st ed., McGraw Hill, New York, 1962.

21. Hertz, H., Miscellaneous Papers, Part V - The Contact of Elastic Solids, The MacMillan Company (London), 1896, pp. 146-162.

22. Roark, R. J. and Young, W. C., Formulas for Stress and Strain, 5th ed., McGraw-Hill, New York, 1975.McGraw-Hill, New York, 1975.

TABLE I. - DISPLACEMENTS AT CORNER NODES OF FINE MESH REGION

[Displacement, mm (in.)]

Node	Case 1 3x9 mesh	Case 2 5x9 mesh	Case 3 10x9 mesh
A	6.63905×10^{-4} (2.61380×10^{-5})	6.63844×10^{-4} (2.61356×10^{-5})	6.63997×10^{-4} (2.61416×10^{-5})
B	6.55147×10^{-4} (2.57932×10^{-5})	6.55881×10^{-4} $(2.582210 \times 10^{-5})$	6.56245×10^{-4} (2.58364×10^{-5})
C	5.99006×10^{-4} (2.35829×10^{-5})	5.99366×10^{-4} (2.35971×10^{-5})	5.99427×10^{-4} (2.35995×10^{-5})
D	6.52635×10^{-4} (2.56943×10^{-5})	6.53811×10^{-4} (2.57406×10^{-5})	6.53964×10^{-4} (2.57466×10^{-5})

TABLE II. - SPUR GEAR DATA

[Gear tolerance per ASME class 12.]

Number of teeth	28
Diametral pitch	8
Circular pitch, cm (in.)	0.9975 (0.3927)
Whole depth, cm (in.)	0.762 (0.300)
Addendum, cm (in.)	0.318 (0.125)
Chordal tooth thickness reference, cm (in.)	0.485 (0.191)
Pressure angle, deg	20
Pitch diameter, cm (in.)	8.890 (3.500)
Tooth width, cm (in.)	0.625 (0.250)
Outside diameter, cm (in.)	9.525 (3.750)
Root fillet, cm (in.)	0.102 to 0.152 (0.04 to 0.06)
Measurement over pins, cm (in.)	9.603 to 0.630 (3.7807 to 3.7915)
Pin diameter, cm (in.)	9.549 (0.216)
Backlash reference, cm (in.)	0.0254 (0.010)
Tip relief, cm (in.)	0.001 to 0.0015 (0.0004 to 0.0006)
Young's modulus, N/m^2 (psi)	2.07×10^{11} (30×10^6)
Poisson's ratio	0.30

TABLE III. - RESULTS OF FEM CALCULATION FOR TOOTH DEFLECTION NORMAL TO THE TOOTH SURFACE AT POINTS ALONG THE LINE OF ACTION

[NASA test gear.]

Roll angle		Distance from pitch point along line of action		Load		Deflection	
rad	deg	mm	in.	N	lb	mm	in.
0.2208	12.65	-5.979	-0.2354	93.05	20.92	5.7412 E-4	2.2603 E-5
.2271	13.01	-5.718	-.2251	238.4	53.59	1.5026 E-3	5.9158 E-5
.2361	13.53	-5.342	-.2103	446.1	100.3	2.8184 E-3	1.1096 E-4
.2474	14.17	-4.867	-.1916	706.8	158.9	4.5072 E-3	1.7745 E-4
.2609	14.95	-4.308	-.1696	1018	228.9	6.5641 E-3	2.5843 E-4
.2760	15.81	-3.673	-.1446	1366	307.2	8.9797 E-3	3.5353 E-4
.2922	16.74	-2.997	-.1180	1615	363.0	1.0875 E-2	4.2813 E-4
.3084	17.67	-2.322	-.0914	1615	363.0	1 1200 E-2	4.4095 E-4
.3238	18.55	-1.676	-.0660	1615	363.0	1.1554 E-2	4.5488 E-4
.3386	19.40	-1.057	-.0416	1615	363.0	1.1930 E-2	4.6970 E-4
.3529	20.22	-.462	-.0182	1615	363.0	1.2345 E-2	4.8603 E-4
.3640	20.86	0	0	1615	363.0	1.2600 E-2	4.9605 E-4
.3747	21.47	.447	.0176	1615	363.0	1.3035 E-2	5.1320 E-4
.3876	22.21	.986	.0388	1615	363.0	1.3501 E-2	5.3155 E-4
.4000	22.92	1.506	.0593	1615	363.0	1.4004 E-2	5.5135 E-4
.4121	23.61	2.012	.0792	1615	363.0	1.4537 E-2	5.7233 E-4
.4237	24.28	2.497	.0983	1615	363.0	1.5090 E-2	5.9408 E-4
.4350	24.92	2.969	.1169	1615	363.0	1.5680 E-2	6.1722 E-4
.4458	25.54	3.419	.1346	1508	339.0	1.5132 E-2	5.9573 E-4
.4557	26.11	3.830	.1508	1280	287.7	1.3438 E-2	5.2905 E-4
.4645	26.61	4.199	.1653	1077	272.2	1.1713 E-2	4.6113 E-4
.4723	27.06	4.526	.1782	896.7	201.6	1.0058 E-2	3.9598 E-4
.4793	27.46	4.818	.1897	735.3	165.3	8.5060 E-3	3.3488 E-4
.4855	27.82	5.077	.1999	592.5	133.2	7.0455 E-3	2.7738 E-4
.4909	28.13	5.304	.2088	467.5	105.1	5.6937 E-3	2.2416 E-4
.4956	28.40	5.502	.2166	359.3	80.77	4.4691 E-3	1.7595 E-4
.4997	28.63	5.669	.2232	265.0	59.57	3.3726 E-3	1.3278 E-4
.5031	28.83	5.812	.2288	186.2	41.87	2.4210 E-3	9.5315 E-5
.5059	28.99	5.928	.2334	121.7	27.35	1.6135 E-3	6.3525 E-5
.5080	29.11	6.017	.2369	73.21	16.46	9.6342 E-4	3.7930 E-5

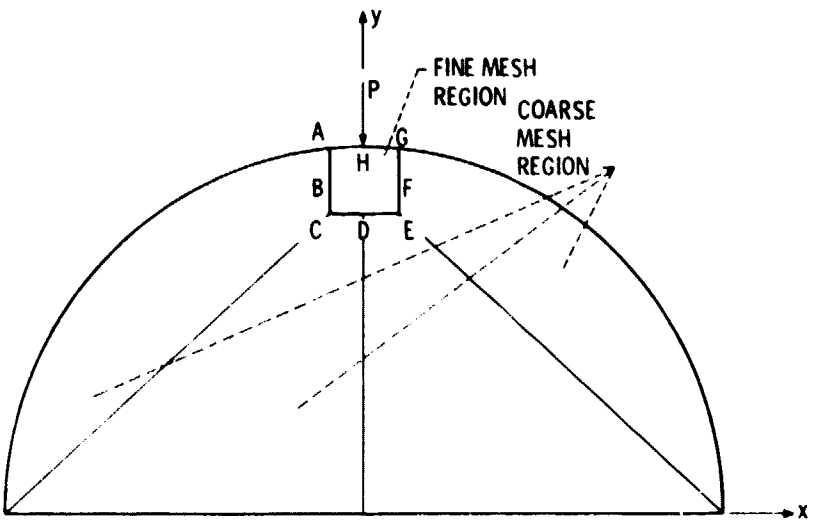

Figure 1. - Finite element model of half cylinder. Zone of fine mesh near point of load application.

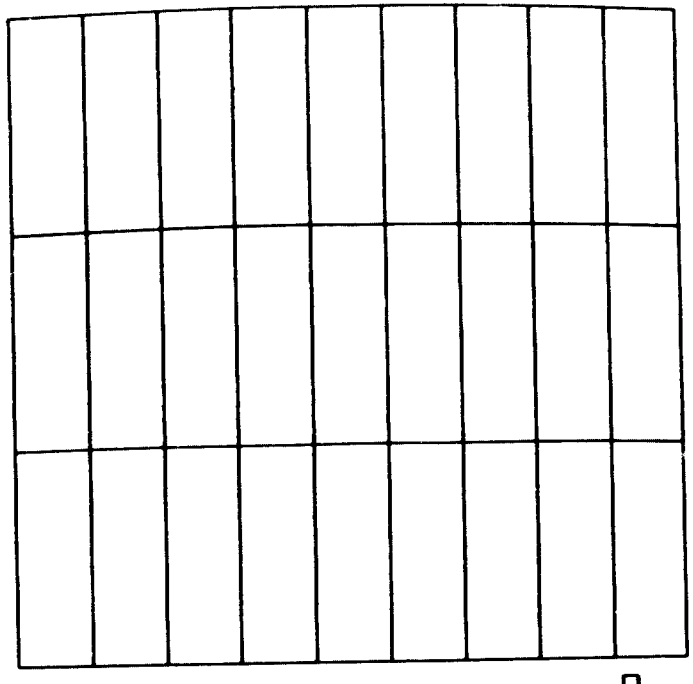

(a) CASE 1, 3x9 MESH, FINE REGION.

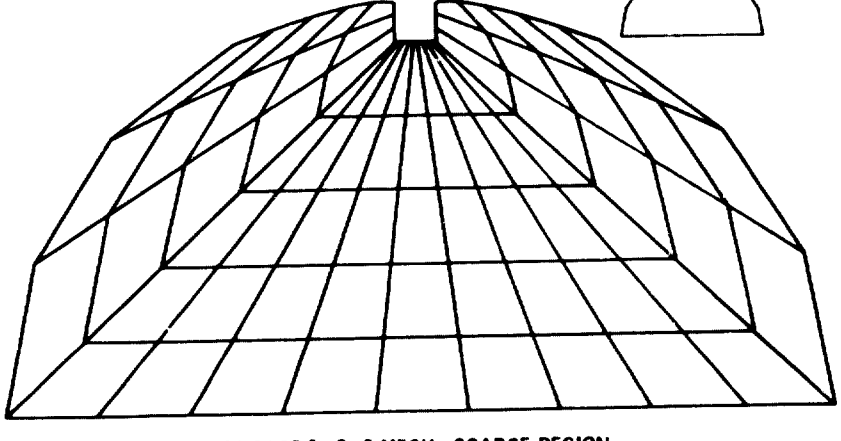

(b) CASE 1, 3x9 MESH, COARSE REGION.

Figure 2. - Finite element model for half cylinder with different mesh arrangements. Fine mesh region is held constant size.

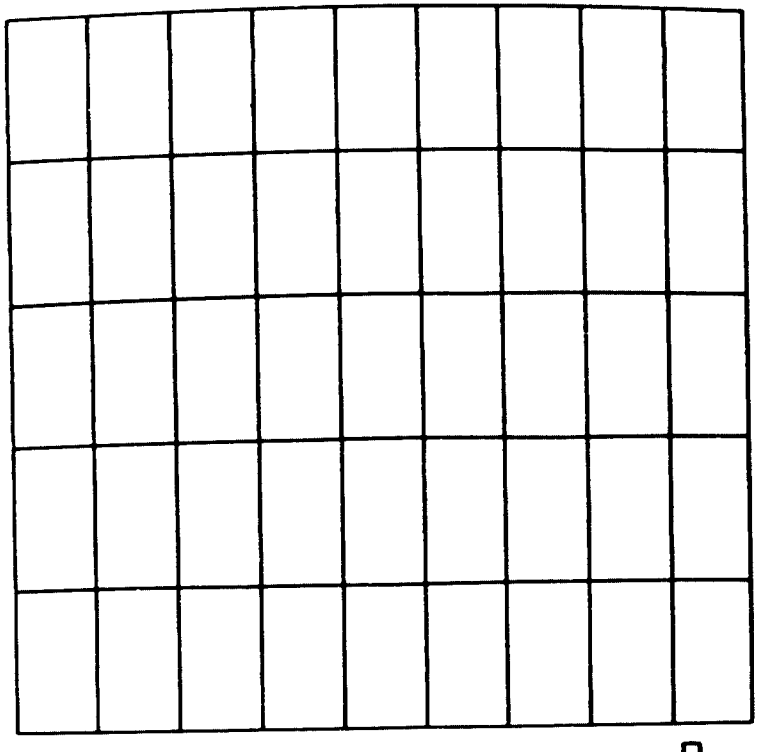

(c) CASE 2, 5x9 MESH, FINE REGION.

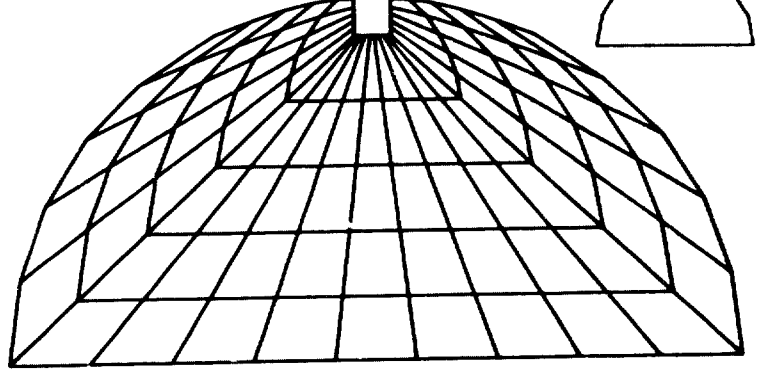

(d) CASE 2, 5x9 MESH, COARSE REGION.

Figure 2. - Continued.

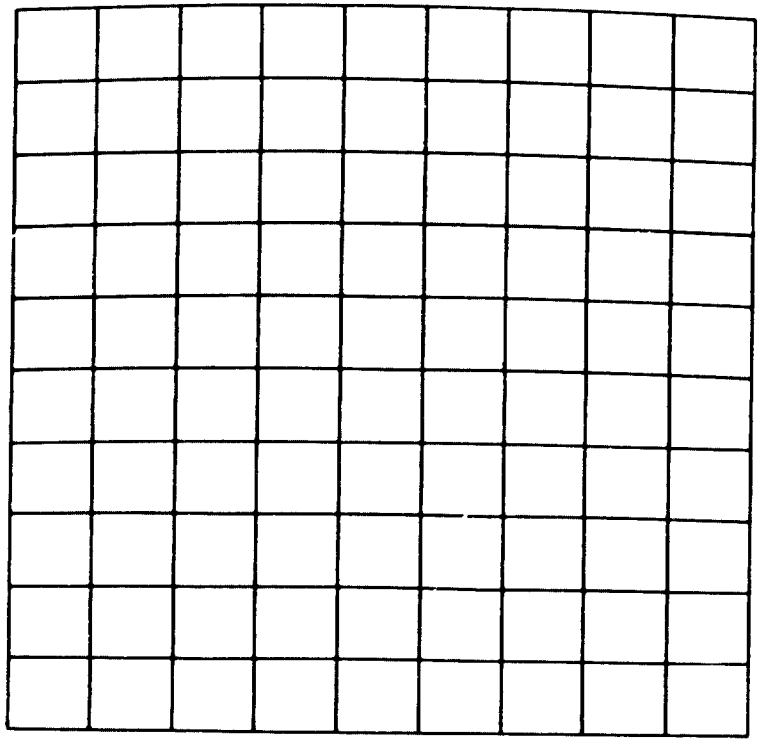

(e) CASE 3, 10x9 MESH, FINE REGION.

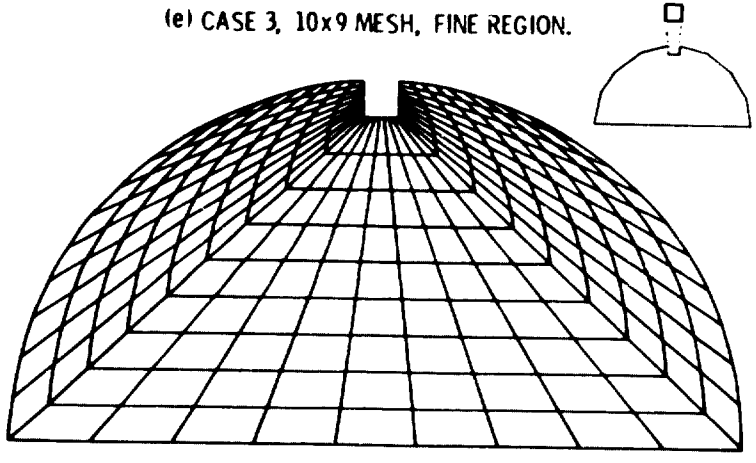

(f) CASE 3, 10x9 MESH, COARSE REGION.

Figure 2. - Concluded.

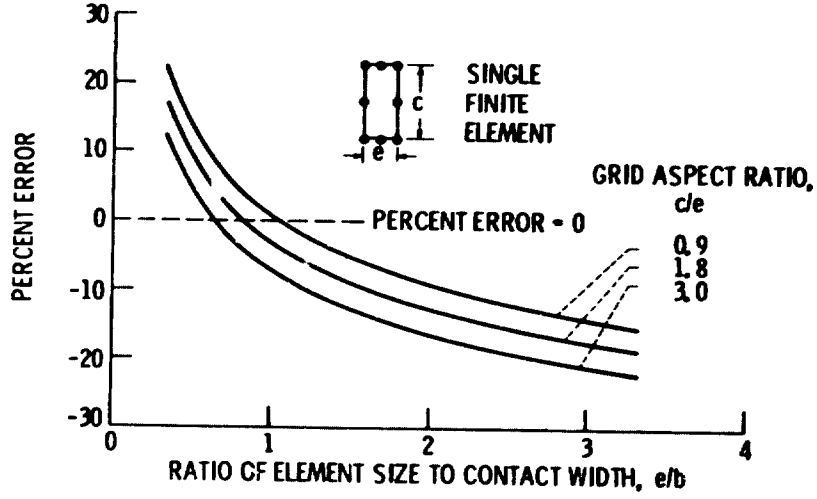

Figure 3. - Deformation of Hertzian line contact by finite element method compared to deformation calculated by the classical Hertz formula.

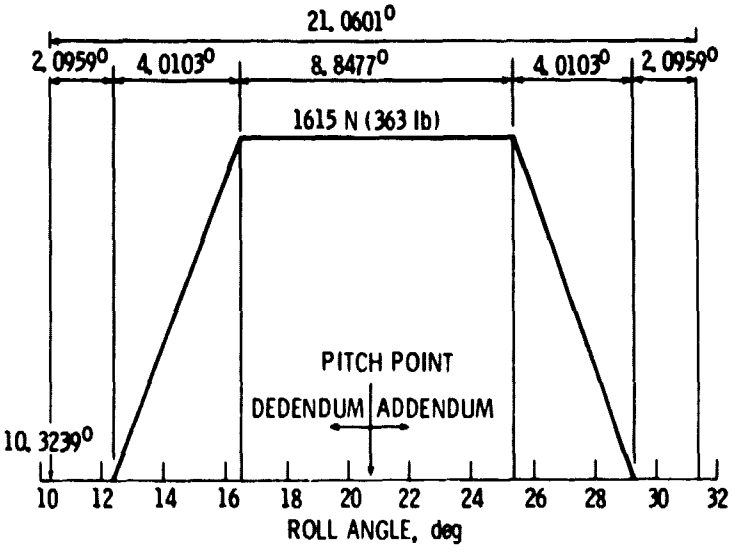

Figure 4. - Loading diagram.

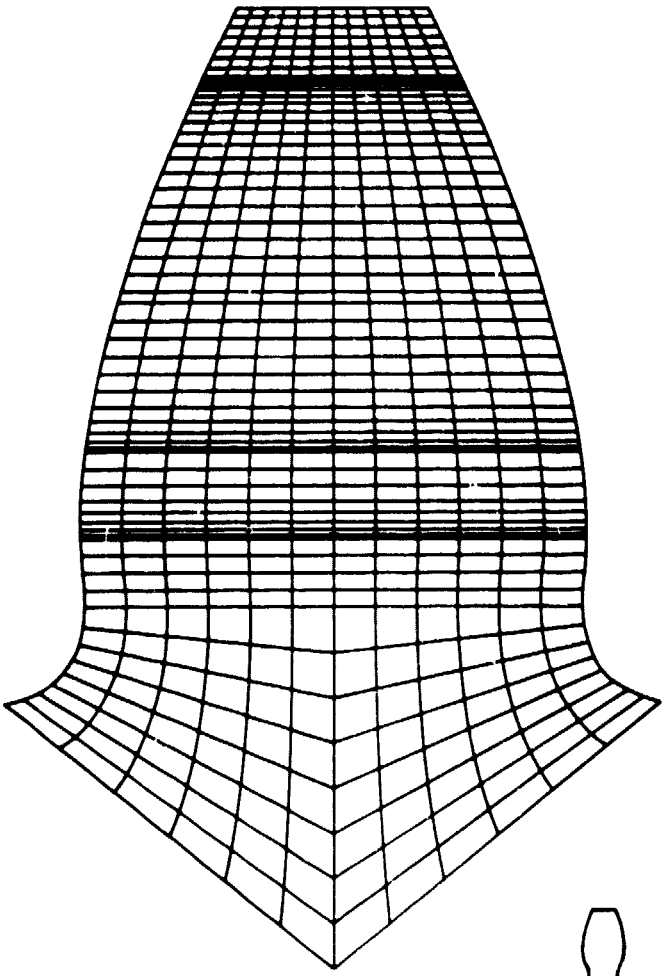

(a) GEAR TOOTH GRID.

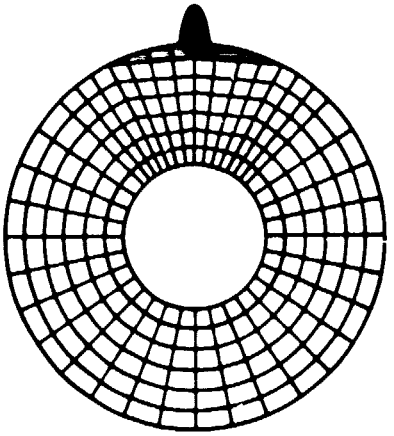

(b) TOOTH AND GEAR BLANK.

Figure 5. - Spur gear mesh.

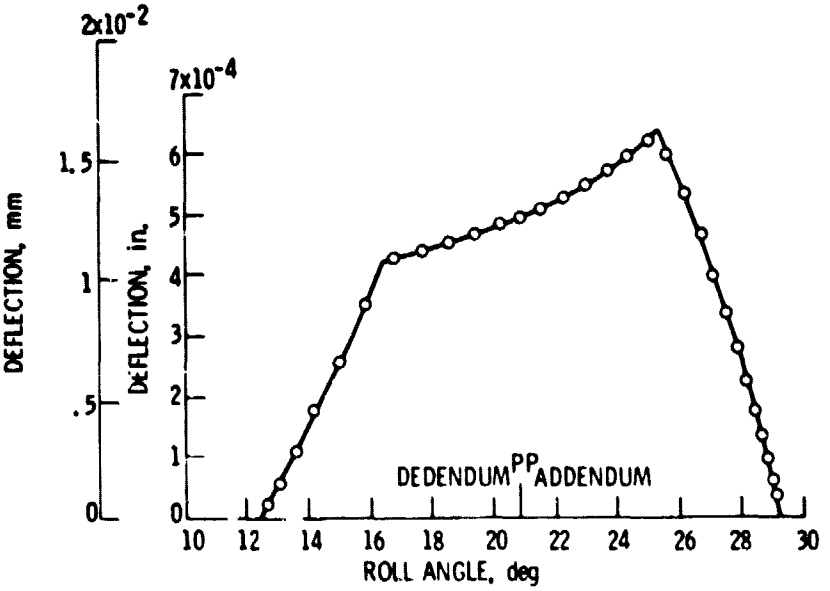

Figure 6. - Results of FEM calculation for tooth deflection normal to the tooth surface at points along the line of action.

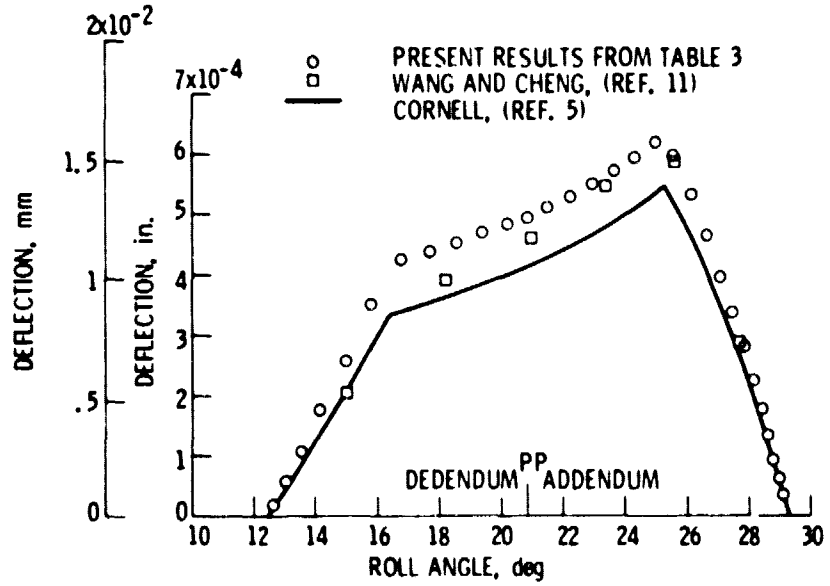

Figure 7. - Results of Wang and Cheng and results of Cornell compared to present results for spur gear deflection.

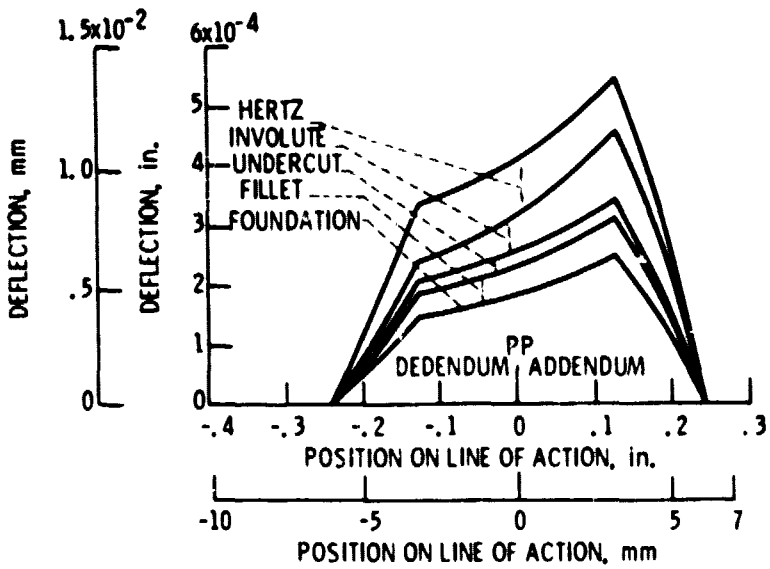

Figure 8. - Tooth deflection calculated by the method of Cornell, reference 5.